# Hydrodynamic long-time tails after a quantum quench

Jonathan Lux,[1,*] Jan Müller,[1] Aditi Mitra,[1,2] and Achim Rosch[1]
[1]*Institut für Theoretische Physik, Universität zu Köln, D-50937 Cologne, Germany*
[2]*Department of Physics, New York University, 4 Washington Place, New York, New York 10003, USA*
(Received 16 December 2013; published 9 May 2014)

After a quantum quench, a sudden change of parameters, generic many-particle quantum systems are expected to equilibrate. A few collisions of quasiparticles are usually sufficient to establish approximately local equilibrium. Reaching global equilibrium is, however, much more difficult as conserved quantities have to be transported for long distances to build up a pattern of fluctuations characteristic for equilibrium. Here we investigate the quantum quench of the one-dimensional bosonic Hubbard model from infinite to finite interaction strength $U$ using semiclassical methods for weak and exact diagonalization for strong quenches. Equilibrium is approached only slowly, as $t^{-1/2}$ with subleading corrections proportional to $t^{-3/4}$, consistent with predictions from hydrodynamics. We show that these long-time tails determine the relaxation of a wide range of physical observables.

DOI: 10.1103/PhysRevA.89.053608 PACS number(s): 05.30.−d, 05.60.−k, 73.43.Cd

## I. INTRODUCTION

States at thermal equilibrium can be described with only a few macroscopic parameters like temperature $T$ and chemical potential $\mu$. The fundamental question of how such an equilibrium state can be reached for an interacting quantum system has recently gained a lot of attention [1–8], partially due to new experimental opportunities to study this question using ultracold atoms. They allow one to realize simple model Hamiltonians and to change their parameters practically instantaneously to study thermalization in a closed quantum system with unprecedented precision and control.

In a typical quantum quench experiment, one considers the evolution of the ground-state wave function $|\Psi_0\rangle$ of an initial Hamiltonian $H_0$ after a sudden change of the Hamiltonian, $H_0 \to H$. The time evolution $|\Psi(t)\rangle = e^{-iHt}|\Psi_0\rangle$ of a many-particle system occurs generically in three main steps: prethermalization, local equilibration, and global equilibration. First the wave function starts to adjust to the new Hamiltonian [4,9] on a short time scale. After this, often a quasistationary "prethermalized" state is obtained [10–13], where quasiparticles have been formed but not yet scattered on each other. Sometimes coherent oscillations characterize this regime for large quenches [14–16]. In a second step, a few scattering processes of the excitation are often sufficient to achieve approximately a local equilibrium state. This can, for example, be captured within a kinetic equation approach [17–19]. Finally the third step, the buildup of a global equilibrium after a quantum quench, has received probably the least attention and will be the focus of this paper. It is dominated by the diffusive transport of conserved quantities, like matter or energy, over large distances. It therefore leads to pronounced long-time tails, well known from hydrodynamics.

Two situations have to be distinguished when studying hydrodynamic long-time tails after a quantum quench: homogeneous and inhomogeneous systems. For example, if the relaxation of ultracold atoms in a trap is considered, in general the spatial distribution of, e.g., the energy will be different before and after the quench. This implies that energy has to be transported over large distances of the order of the size $L$ of the system [20,21]. If this transport is diffusive, this takes a very long time $L^2/D$, where $D$ is a diffusion constant. In Ref. [20] this effect was studied quantitatively for weakly interacting fermions released from a trap. Perhaps more surprisingly, conservation laws and diffusion lead also to extremely slow relaxation in translationally invariant systems studied in the following. Here it is important to realize that any classical or quantum state is characterized by a pattern of fluctuations. Consider, for example, fluctuations of the energy density $\delta e = e - \langle e\rangle$, in a system at $T > 0$, where correlations decay on a finite length scale $l_c$. In equilibrium and on length scales large compared to $l_c$, they can be described by the equal-time correlation function

$$\langle \delta e(\boldsymbol{r})\delta e(\boldsymbol{r}')\rangle_{\rm eq} \approx c_v\, k_B T^2\, \delta(\boldsymbol{r}-\boldsymbol{r}'), \tag{1}$$

where $c_v = (\langle H^2\rangle - \langle H\rangle^2)/(V k_B T^2)$ is the specific heat per volume. During equilibration, the system has to build up this fluctuation pattern; see Fig. 1. If only energy is conserved, one can describe the equilibration at long times by a stochastic linearized diffusion equation [22]

$$\partial_t e - D\nabla^2 e = \nabla f, \tag{2}$$

where $\langle f(\boldsymbol{r},t) f(\boldsymbol{r}',t')\rangle_{\rm eq} = 2Dc_v T^2 \delta(\boldsymbol{r}-\boldsymbol{r}')\delta(t-t')$. As discussed in Appendix A, one obtains from a straightforward solution of this equation in $d$ spatial dimensions

$$\langle \delta e(\boldsymbol{r},t)\delta e(\boldsymbol{r}',t)\rangle - \langle \delta e(\boldsymbol{r})\delta e(\boldsymbol{r}')\rangle_{\rm eq} \sim t^{-d/2} + O(t^{-3d/4}) \tag{3}$$

for $|\vec{r}-\vec{r}'|^2 \ll Dt$. A simple scaling analysis using Eq. (2) as a fixed point (see Appendix A) shows that correction terms [23] to Eq. (2), like $\partial_x(e\partial_x e)$, lead to corrections vanishing as $1/t^{3d/4}$. The same results are obtained when additional diffusive modes (e.g., particle density $n$) are included. The situation is, however, different in systems with momentum conservation. In this case the momentum current (i.e., the pressure) has contributions proportional to $(\delta e)^2$ and $(\delta n)^2$. These are relevant perturbations in dimensions $d < 2$, described by the Kardar-Parisi-Zhang (KPZ) universality class [24–27] in $d = 1$. In this case one expects that some modes relax as $1/t^{2/3}$ instead of $1/t^{1/2}$ as observed numerically [28].

*lux@thp.uni-koeln.de

 

FIG. 1. (Color online) After a quench and subsequent thermalization, the amplitude of local fluctuations of, for example, the energy density changes. As energy has to be transported diffusively over large distances to build up the new pattern of fluctuations, equilibration takes long times, resulting in hydrodynamic long-time tails.

## II. THE MODEL

In this paper we will study a quantum quench in a lattice model without momentum conservation. We consider the one-dimensional (1D) bosonic Hubbard model

$$H = -J\sum_i a_i^\dagger a_{i+1} + \text{H.c.} + \frac{U}{2}\sum_i n_i(n_i-1) \qquad (4)$$

after a sudden quench from an initial state at $U=\infty$ where $n_i = a_i^\dagger a_i = 1$ to a state with finite $U$.

We have chosen this model for four reasons: (i) The bosonic Hubbard model is probably the many-particle model best suited for experimental quench studies using ultracold atoms [7,8,29], (ii) long-time tails are most pronounced in 1D, (iii) the 1D case is especially suited for numerical studies, and, finally, (iv) in contrast to many other simple 1D models, the bosonic Hubbard model is *not* close to an integrable point: the dominant excitations of the bosonic Mott insulator, doublons and holons, have *different* dispersions and can therefore equilibrate by simple two-particle collisions [30].

We first consider a weak quench from $U=\infty$ to a finite but large $U \gg J$. In this limit a dilute gas of quasiparticles, holons (empty sites) with dispersion $\epsilon_k^h \approx -2J\cos k$ and doublons (doubly occupied sites) with energy $\epsilon_k^d \approx -4J\cos k$ are created. As their average separation $\rho^{-1} = 1/4\,(U/J)^2$ [31] is much larger than their typical wavelength, a simple quasiclassical treatment of their dynamics is possible, following Sachdev and Damle [32]. This approach was recently applied to quantum quenches in an integrable system in Ref. [33] and to short-time dynamics in Ref. [31]. While the motion of the quasiparticles can be treated classically, their creation and scattering is a quantum-mechanical process.

## III. SEMICLASSICAL APPROACH

To describe relaxation to equilibrium after the quench, we first calculate the probability $p_k = 8\,(J/U)^2\sin^2 k = \rho[1-\cos(2k)]$ that a doublon-holon pair with momenta $k$ and $-k$ is created at a given site. This probability is used to create at $t=0$ an ensemble of doublons and holons moving with the velocities $\partial_k\epsilon_k^d$ and $\partial_k\epsilon_k^h$, respectively. The position and the time of the next scattering event can then be determined successively. Doublon-doublon and holon-holon scattering have no effect

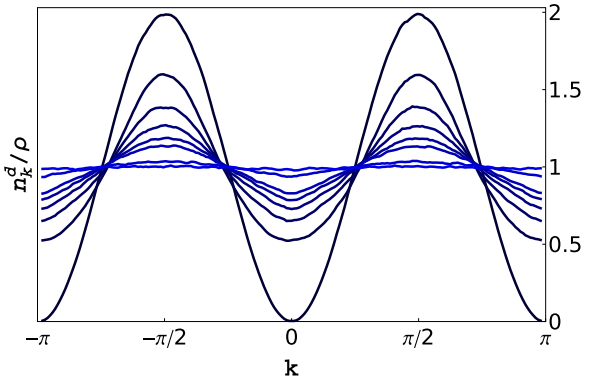


FIG. 2. (Color online) Doublon momentum distribution function for times $t = (0,1,2,3,4,5,10,20)\tau_{dh}$ after the quench, where $\tau_{dh}$ is the doublon-holon scattering time, and $\rho = 4(J/U)^2$ is the doublon density. For $t\to\infty$ an equilibrium state at $T=\infty$ is approached where all momenta are equally occupied.

(as only the momenta of the two particles are exchanged), while the scattering of holons and doublons leads to relaxation. To leading order in $U \gg J$ the reflection probability is 1 and the new momenta after scattering can just be calculated from energy and lattice-momentum conservation. Repeating this procedure, we track the motion of about $10^5$ quasiparticles for long times and, furthermore, average over 500 ensembles. Correlation functions obtained by this semiclassical dynamics are expected to give the corresponding quantum-mechanical correlation functions for $U \gg J$ [32]. Related models of hard-core particles moving in 1D have also been simulated, e.g., in Refs. [28,34,35] to study thermal transport. In contrast to our case, however, quadratic dispersions and momentum conservation were used. We have also implemented a version which takes into account the finite tunneling probability of doublons and holons of order $(J/U)^2$, but as qualitatively similar results have been obtained in this case, we show results only for vanishing tunneling rate in the following.

In Fig. 2 we show how the momentum distribution of doublons gets flatter and flatter as a function of time. As the initial total kinetic energy is on average zero, the system relaxes toward an equilibrium state at $T=\infty$. For all semiclassical plots we measure the time scale in units of $\tau_{dh} \approx 0.031U^2/J^3 = 0.123\rho^{-1}/J$, the doublon-holon scattering time (obtained by dividing the simulated time by the total number of doublon-holon scattering events and the number of doublons). In these units, all semiclassical results are completely independent of $U/J$.

Note that the semiclassical approach does not contain extremely rare processes where a holon-doublon pair is created or annihilated by converting the kinetic energy of a large number of quasiparticles (of order $U/J$) into interaction energy in a complicated process [36]. We will not consider the exponentially (in $U/J$) long time scales [36] where these processes become important and which ultimately lead to an equilibrium state with $J \ll T < \infty$.

While we will argue that hydrodynamic long-time tails generically govern the relaxation of most physical observables for $t\to\infty$, we find that they are much more pronounced in some observables. We obtain the most pronounced long-time

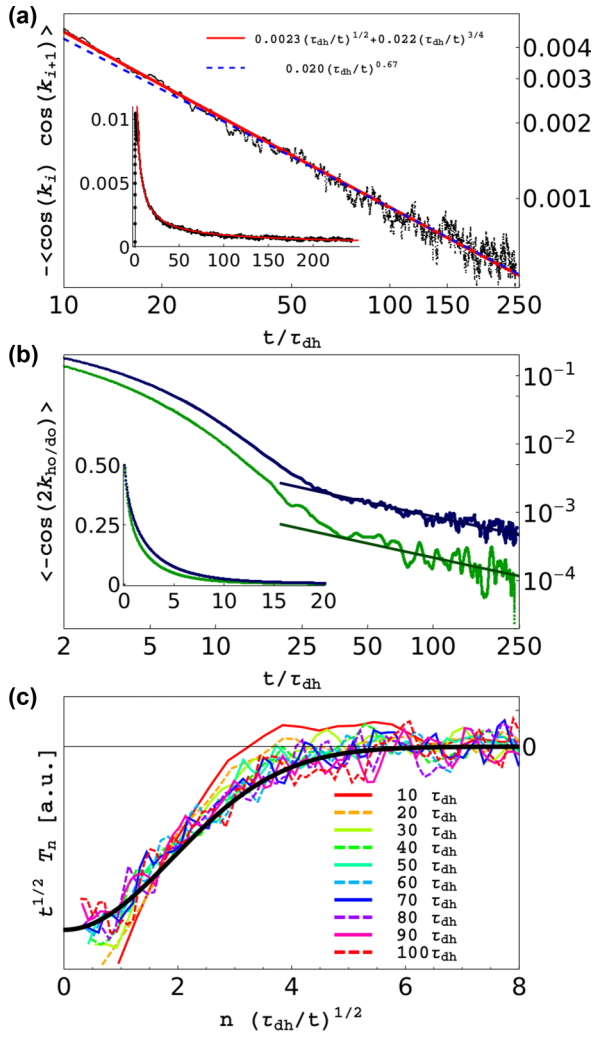


FIG. 3. (Color online) (a) The decay of the energy-energy correlation function of nearest-neighbor quasiparticles is very slow in time and consistent with hydrodynamic predictions. (b) Expectation value of $-\cos(2k)$ for doublons (dark blue) and holons (light green). Initially these quantities decay approximately exponentially in a few collisions. At long times, however, a hydrodynamic long-time tail is visible. The solid lines are quantitative predictions of these long-time tails, obtained from the fit to the upper plot using Eq. (10). (c) Scaling plot of $T_n$, Eq. (5). The thick black line is Eq. (6) with $D_e$ evaluated from the Kubo formula.

tails for the correlation functions

$$T_n(t) = \langle \cos k_i(t) \cos k_{i+n}(t) \rangle \tag{5}$$

describing the energy-energy correlation function of particle $i$ and particle $i+n$ (we enumerate the particles from left to right). Within a simple Boltzmann equation treatment of the problem (see Appendix B), this quantity vanishes. The solid line in Fig. 3(a) shows a fit to $T_1(t)$ of the form $c_1/t^{1/2} + c_2/t^{3/4}$, consistent with Eq. (3). Note that it is mandatory to include subleading corrections to the fit as those are suppressed only by relative factors of $1/t^{1/4}$. From a simple power-law fit $ct^{-\alpha}$ (dashed line), one obtains $\alpha \approx 0.67$ which describes the numerical data equally well. While this exponent is reminiscent of the 2/3 expected for the KPZ universality class, we believe that this agreement is only accidental, as strong umklapp scattering relaxes the current rapidly, which is inconsistent with the KPZ universality class (see above). At least three orders of magnitude longer simulations are needed to be able to distinguish numerically the different asymptotic behaviors. A similar discussion of an equilibrium correlation function is given in Appendix C.

To investigate how the hydrodynamic correlations spread in space, we show in Fig. 3(c) a scaling plot of $\sqrt{t}T_n(t)$ as a function of $n/\sqrt{t}$ at different times. The approximate scaling collapse for long times shows that the information spreads diffusively, $n \sim \sqrt{t}$. From linear hydrodynamics, Eq. (2), one can easily calculate the scaling function (see Appendix A)

$$T_n(t) \sim \frac{1}{\sqrt{t}} \exp\left(-\frac{n^2}{8\tilde{D}_e t/\tau_{dh}}\right). \tag{6}$$

While the prefactor, depending on details of the quench, is unknown, the energy diffusion constant $\tilde{D}_e = D_e \tau_{dh} \rho^2 \approx 0.91$ can be calculated from the Kubo formula evaluated at thermal equilibrium. The thick black line in Fig. 3(c) shows that the analytic formula describes the data quantitatively. This shows that indeed linear hydrodynamics governs the buildup of long-time tails.

When investigating the relaxation of the momentum distribution, such long-time tails are much more difficult to detect. In Fig. 3(b), we show the expectation value of $\cos(2k)$ for doublons and holons,

$$T^{d,h}(t) = \left\langle \cos\left(2k_i^{d,h}\right)\right\rangle, \tag{7}$$

where the expectation value is determined by summing over only doublon or holon momenta, respectively. Up to a normalizing factor, this is the dominant Fourier component of the distribution function shown in Fig. 3(b). As $\cos^2 k = (1 + \cos 2k)/2$, it is also directly related to the square of the kinetic energy of each particle. At first, $T^{d,h}$ decays exponentially on time scales consistent with predictions from the Boltzmann equation; see Appendix B. For $t \gtrsim 25\,\tau_{dh}$, however, a small but finite long-time tail dominates the relaxation.

The relative prefactors of the long-time tail in various physical quantities are related to each other as they arise from the same hydrodynamic modes. To predict analytically how the prefactors are related, we recall their physical origin: after a *local* equilibrium has been established, it takes a long time to establish *globally* the characteristic fluctuations of the conserved densities. We therefore investigate first how *in thermal equilibrium* the observables $T_{1,\mathrm{eq}}, T^d_{\mathrm{eq}}$, and $T^h_{\mathrm{eq}}$, defined in Eqs. (5) and (7), depend on the densities $n^d$ and $n^h$ and the energy per particle $\epsilon$. In the semiclassical limit the distribution functions are given by $n_k^{d,h} = z_{d,h} e^{-\beta\epsilon_k^{d,h}}$, where the fugacities $z_d$ and $z_h$ and $\beta = 1/T$ are functions of $n^d$, $n^h$, and $\epsilon$, and we consider the limit $\beta J \ll 1$. Expectation values for doublons and holons can be calculated from $\langle O\rangle_{d,h} = \int \frac{dk}{2\pi}\, O(k)\, n_k^{d,h}$. As doublons and holons are created in pairs, their densities are equal: $n^d = \langle 1\rangle_d = n^h = \langle 1\rangle_h = \rho$. Therefore the energy per particle

$$\epsilon = \frac{\langle \epsilon^d\rangle_d + \langle \epsilon^h\rangle_h}{n^d + n^h} = -5\beta J^2 + O(J(\beta J)^3) \tag{8}$$

is only a function of $\beta$.

Similarly, the three observables $T_{1,\mathrm{eq}}, T^d_{\mathrm{eq}}$, and $T^h_{\mathrm{eq}}$ depend only on $\beta$. Using Eq. (8), they can therefore be written as functions of $\epsilon$ only:

$$T_{1,\mathrm{eq}} \approx \frac{17}{200}\left(\frac{\epsilon}{J}\right)^2,$$
$$T^d_{\mathrm{eq}} \approx \frac{16}{200}\left(\frac{\epsilon}{J}\right)^2, \tag{9}$$
$$T^h_{\mathrm{eq}} \approx \frac{4}{200}\left(\frac{\epsilon}{J}\right)^2.$$

The fact that these observables depend only on $\epsilon$ arises only for models without forces where the energy is independent of the distance of particles. Equation (9) shows that the three observables are sensitive to fluctuations of the energy but insensitive to fluctuations of the densities. Therefore we expect that only the relaxation of a single mode, the energy fluctuations, will dominate the equilibration of all three quantities. Furthermore, the prefactor of the long-time tails will directly be proportional to the prefactors obtained in Eq. (9). We can use this to predict analytically the *relative* prefactors of the long-time tails

$$T^d = \frac{16}{17}T_1, \quad T^h = \frac{4}{17}T_1 \quad \text{for } t \to \infty, \tag{10}$$

fully consistent with our numerical results, as shown by the solid lines in Fig. 3.

## IV. EXACT DIAGONALIZATION

The semiclassical approach discussed above breaks down for strong quenches when the distance of quasiparticles becomes comparable to their wavelength. To analyze this regime we have used the ALPS code [37] for brute-force exact diagonalization of small systems to investigate the relaxation to equilibrium. The initial state, a perfect Mott insulator ($U = \infty$ or $J = 0$), is a product state where each site is singly occupied. We then performed a sudden change of parameters to $U = J$. This corresponds to a strong quench—the initial state is not close to an eigenstate. For our numerics, we use periodic boundary conditions, and we do not include states in the Hilbert space where three or more bosons occupy a single site. Hence our results describe a modified Hubbard model with a large three-particle term $U' \sum_i n_i(n_i - 1)(n_i - 2)$. This allows us to reach larger system sizes.

Even for this fully quantum-mechanical calculation we obtain strong evidence of hydrodynamic long-time tails; see Figs. 4 and 5. The clearest signature is obtained for the nearest-neighbor correlation function of doubly occupied sites, Fig. 4, which directly contributes to the energy-energy correlation function. For small system sizes with only $L = 10$ sites, strong finite-size effects do not allow us to identify how the long-time average is approached. For slightly larger systems, however, one can clearly see in Fig. 4 that the steady state is approached very slowly, consistent with a power-law tail. While it is not possible to extract from this data set reliably any exponent (see the various fits in Figs. 4 and 5) or perform a meaningful scaling

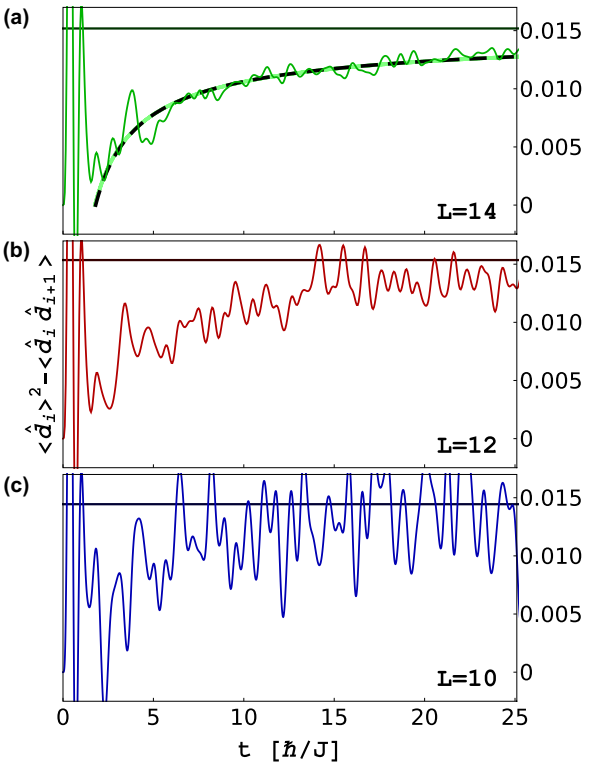


FIG. 4. (Color online) Time evolution of the nearest-neighbor doublon correlations $-\langle \hat{d}_i \hat{d}_{i+1}\rangle + \langle \hat{d}_i\rangle^2$ with $\hat{d}_i = n_i(n_i - 1)/2$ obtained from exact diagonalization data for system sizes $L = 14, 12, 10$ after a quench from $U = \infty$ to $U = J$. The solid lines are the long-time averages obtained for each system size separately. For $L = 14$ two fitting functions are shown. The black dashed line $-0.022\,(Jt)^{-0.69}$ is the best fit using a single exponent only, while the green solid line $-0.0033\,(Jt)^{-1/2} - 0.02\,(Jt)^{-3/4}$ is of the form as expected from hydrodynamics; see Appendix A.

analysis, the results are clearly consistent with the type of long-time tails expected from hydrodynamics. It is important to note that also in the prethermalization regime of quantum quenches, i.e., on time scales *smaller* than the scattering time of quasiparticles, one obtains power-law relaxation as has been shown by Barmettler *et al.* [31] in a study of the collisionless dynamics of doublons and holons in the Bose-Hubbard model. As we expect that scattering times for our parameters (strong quench to $U = J$) are short, we believe that the slow relaxation observed in Fig. 4 occurs on time scales considerably *larger* than the scattering time. Therefore the observed long-time tails are very likely of hydrodynamic origin. Also the number of doubly occupied sites (Fig. 5), which can directly be measured experimentally [36], shows clear indications of long-time tails.

It is surprising that the slow relaxation is so pronounced already in a 14-site systems: often finite-size effects dominate for such small systems and long times. Here it helps that diffusive transport is much slower than ballistic transport. The typical time scale associated with diffusive transport over $L$ sites scales with $L^2$. As $14^2 = 196$, it is not surprising that diffusive effects dominate on the simulated time scales.

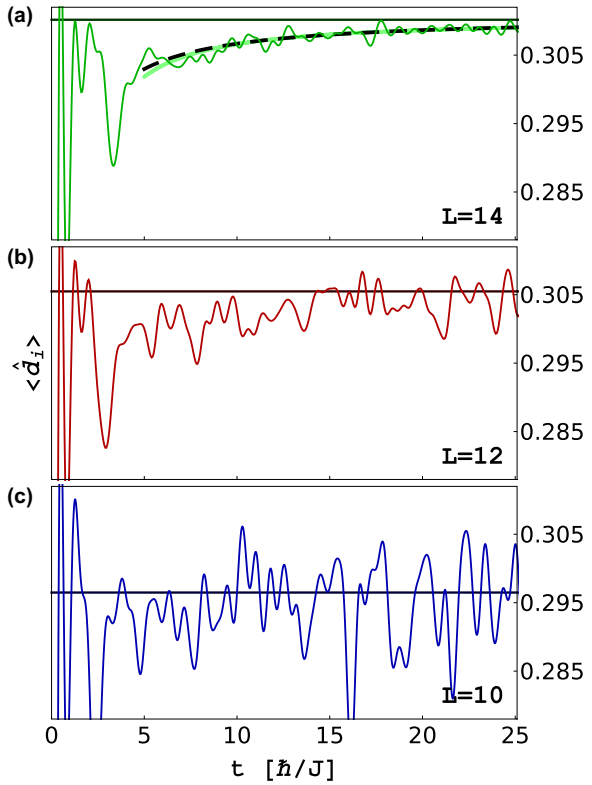


FIG. 5. (Color online) Time evolution of the number of doublons per site $\langle \hat{d}_i \rangle = \langle n_i(n_i-1)/2 \rangle$ obtained from exact diagonalization data for system sizes $L = 14,12,10$ after a quench from $U = \infty$ to $U = J$. The solid lines are the long-time averages obtained for each system size separately. For $L = 14$ two fitting functions are shown. The black dashed line $-0.06\,(Jt)^{-1.23}$ is the best fit using a single exponent only, while the green solid line $0.016(Jt)^{-1/2} - 0.048(Jt)^{-3/4}$ is of the form expected from hydrodynamics; see Appendix A.

## V. CONCLUSION AND OUTLOOK

Studying in detail the equilibration within the one-dimensional Bose-Hubbard model, we have demonstrated the importance of algebraic long-time tails for the relaxation in a closed quantum system. Our numerical results for strong quenches as well as for weak quenches are fully consistent with predictions from hydrodynamics. The hydrodynamic long-time tails govern the relaxation of practically all physical observables in generic quantum and classical many-particle systems as long as a small number of conservation laws are present. The relevance of these long-time tails depends strongly on the observable which is considered. Sometimes they are difficult to observe due to tiny prefactors. Unexpectedly, the long-time tails turned out to be more pronounced in the quantum regime compared to the semi-classical limit: while we needed billions of classical hard-core collisions to identify them, they are clearly visible in a tiny quantum system. The reason might be the more complex interaction processes in a many-particle quantum system.

How can one can engineer an interacting many-particle system which relaxes rapidly to an equilibrium state? This is an interesting question especially as in experiments with ultra-cold atoms, loss processes often put severe limits on achievable time scales. Our results show that increasing the scattering rate might not be the best way to achieve fast relaxation as this typically leads to smaller diffusion constants. As a consequence, it will take longer to build up the fluctuations characteristic for a global equilibrium state and the hydrodynamic long-time tails will have larger prefactors. For the future it will be interesting to study how not only the scattering processes but also the rate of change of parameters in the system influence the role of hydrodynamic long-time tails.

## ACKNOWLEDGMENTS

It is a pleasure to thank M. Becker, P. Bröcker, C. Kolllath, J. Krug, W. Michel and, especially, H. Spohn for helpful discussions. The simulations were performed on the CHEOPS cluster at RRZK Köln. This work was supported by NSF-DMR Grant No. 1303177 (A.M.), the Simons Foundation (A.M.), and the SFB TR12 of the DFG.

## APPENDIX A: LONG-TIME TAILS IN LINEAR HYDRODYNAMICS

In this appendix we briefly review the origin of long-time tails after a quench in systems without momentum conservation. While all results presented in this section are well known, we have not been able to find an appropriate reference. For simplicity we restrict the discussion to a single conserved quantity, the energy. The hydrodynamic equations can easily be generalized to several diffusive modes by replacing the energy density $e$ by a vector of conserved densities, the diffusion constant by a diffusion tensor, and the specific heat by a matrix of thermodynamics susceptibilities (for the semiclassical calculation discussed in the main text energy does not couple to the other conservation laws; see below). The qualitative results remain unmodified as long as all diffusion constants are finite, only conservation laws even under time reversal and parity are considered, and, most importantly, momentum is not conserved.

The starting point is the linearized stochastic diffusion equation in $d$ dimensions [22]

$$\partial_t e - D_e \nabla^2 e = \nabla \mathbf{f}, \tag{A1}$$

where $D_e$ is the energy diffusion constant and $f_i$ describes thermal fluctuations of the energy current. The size of fluctuations can be determined from the condition that the equilibrium correlations of the energy are correctly reproduced by Eq. (A1),

$$\langle e(r)e(r')\rangle_{\mathrm{eq}} = c_V k_B T^2 \delta(r-r'), \tag{A2}$$

where $c_V$ is the the specific heat per volume. In reality, these correlations are not exactly local but as the hydrodynamic equations describe only the behavior at long time and length scales, we can approximate the spatial correlations by a $\delta$ function. One obtains therefore that the fluctuations of the current

$$\langle f_i(r,t) f_j(r',t')\rangle = \delta_{ij} 2k_B T^2 c_V D_e \delta(r-r')\delta(t-t') \tag{A3}$$

are proportional to both the diffusion constant and the specific heat.

For a given initial condition $e(r,0) = e_0(r)$, Eq. (A1) is solved for $t \geqslant 0$ by

$$e(r,t) = \int d^d r'\, g_{D_e}(r-r',t) e_0(r') + \int_0^t dt' \int d^d r'\, g_{D_e}(r-r',t-t') \nabla \mathbf{f}(r',t'), \quad \text{(A4)}$$

$$g_{D_e}(r,t) = \frac{1}{(4\pi D_e t)^{d/2}} \exp\left(-\frac{r^2}{4D_e t}\right). \quad \text{(A5)}$$

From this solution and Eq. (A3) one obtains directly the relaxation of the energy fluctuations as a function of time

$$\langle e(r,t)e(r',t)\rangle - \langle e(r)e(r')\rangle_{\text{eq}} = \int d^d r_1 d^d r_2\, g_{D_e}(r-r_1,t) g_{D_e}(r'-r_2,t) \times \left(\langle e_0(r_1)e_0(r_2)\rangle - \langle e(r_1)e(r_2)\rangle_{\text{eq}}\right). \quad \text{(A6)}$$

This equation describes how the fluctuations of energy approach their equilibrium value. As generically the energy fluctuations directly after a quench, $\langle e_0(r)e_0(r')\rangle$, will differ from their expectation value in the long-time limit, they have to be built up slowly by diffusive transport.

Assuming sufficiently short-ranged correlations in the initial state and using that $\int dr_1 g_D(r-r_1,t) g_D(r'-r_1,t) = g_{2D}(r-r',t)$, one obtains from Eqs. (A5) and (A6)

$$\langle e(r,t)e(r',t)\rangle - \langle e(r)e(r')\rangle_{\text{eq}} \sim \frac{1}{t^{d/2}} \exp\left(-\frac{(r-r')^2}{8D_e t}\right). \quad \text{(A7)}$$

After a quench, one therefore approaches the global equilibrium state only algebraically. Corrections to this formula from nonlinear contributions are discussed below. In Fig. 3 of the main text, we show that the spread of correlations in our semiclassical simulations indeed follows Eq. (A7); see the solid line in Fig. 3(c) To obtain a quantitative fit, we have determined the diffusion constant $D_e$ from the heat conductivity $\kappa$ using

$$D_e = \kappa \left(\frac{\partial \langle e\rangle_{\text{eq}}}{\partial T}\right)^{-1} = \kappa \left(\frac{1}{k_B T^2} \sum_i \rho_i \langle e_i^2\rangle_{\text{eq}}\right)^{-1} \quad \text{(A8)}$$

where the sum runs over the two particle species with density $\rho_i$. The thermal conductivity $\kappa$ can be determined numerically using the Kubo formula [38]

$$\kappa = \frac{1}{L k_B T^2} \int_0^\infty dt \langle J_e(t) J_e(0)\rangle_{\text{eq}} \quad \text{(A9)}$$

where $J_e$ is the total energy current, and $L$ is the system size. For our semiclassical simulations we have to consider the $T \to \infty$ limit. Note that $D_e$ is finite in this limit as all factors of $T$ cancel. Furthermore, all linear thermoelectric effects, i.e., the coupling of the energy current to gradients of the particle density vanish in this limit (nonlinear couplings do, however, exist; see below) which justifies the use of energy diffusion only in the derivation of Eq. (A7).

To estimate the importance of corrections to the linear stochastic diffusion equation, it is useful to perform a simple scaling analysis. Equation (A1) is invariant under the scaling transformation $x \to \tilde{x}$, $t \to \tilde{t}$, $f \to \tilde{f}$, and $e \to \tilde{e}$ with

$$x = \lambda \tilde{x}, \quad t = \lambda^2 \tilde{t}, \quad e = \frac{1}{\lambda^{d/2}} \tilde{e}, \quad f = \frac{1}{\lambda^{(d+2)/2}} \tilde{f}. \quad \text{(A10)}$$

The analogous scaling relations also apply for the density $n$ and the fluctuations of the charge current. Examples of possible correction terms are $\alpha \nabla(e \nabla e)$, $\alpha' \nabla(n \nabla e)$, or $\beta \nabla^4 e$. Rewriting those in the new variables, one finds that they are suppressed for large $\lambda$, $\tilde{\alpha} = \alpha/\lambda^{d/2}$, $\tilde{\alpha}' = \alpha/\lambda^{d/2}$, and $\tilde{\beta} = \beta/\lambda^2$ (reflecting the scaling dimensions of $e$ and $\nabla^2$, respectively). The relaxation after a quantum quench is therefore expected to be of the form

$$\begin{aligned}\langle e(r,t)e(r',t)\rangle - \langle e(r)e(r')\rangle_{\text{eq}} &\sim \frac{1}{\sqrt{t}} f\left(\frac{r}{\lambda}, \frac{t}{\lambda^2}, \frac{\alpha}{\lambda^{d/2}}, \frac{\alpha'}{\lambda^{d/2}}, \frac{\beta}{\lambda^2}, \dots\right) \\ &= \frac{1}{\sqrt{t}} f\left(\frac{r}{\sqrt{t}}, 1, \frac{\alpha}{t^{d/4}}, \frac{\alpha'}{t^{d/4}}, \frac{\beta}{t}, \dots\right), \end{aligned} \quad \text{(A11)}$$

where $f$ is a scaling function, the ellipses denote further subleading corrections, and we have set $\lambda = \sqrt{t}$ in the last equality. Using a Taylor expansion in the last three arguments for large $t$, one finds that corrections are suppressed by $\alpha/t^{d/4}$, $\alpha'/t^{d/4}$, and $\beta/t$. In our model, the $\alpha$ term is absent at $T = \infty$ due to the $e \to -e$ symmetry. The $\alpha'$ term, however, should be present. Note that nonlinearities of the form $\nabla e^2$ arising as corrections to the momentum current in systems with momentum conservation are instead relevant perturbations in $d = 1$ leading to the KPZ universality class [24,27]. Such a term cannot arise as a correction to the energy or charge current as it would violate inversion symmetry. A related discussion of how subleading nonlinearities affect the optical conductivity of metals without momentum conservation has been given in Ref. [23].

## APPENDIX B: BOLTZMANN EQUATION IN THE SEMICLASSICAL REGIME

For weak quenches, $U \gg J$, the density of of excitations, doublons and holons, induced by the quench is very low. It is instructive to investigate their relaxation within the Boltzmann approach. This approach can describe local equilibration but does not reproduce hydrodynamic long-time tails in homogeneous systems.

Denoting the semiclassical distribution functions of doublons and holons as $n_k^d$ and $n_k^h$, respectively, the Boltzmann equation takes the form

$$\frac{\partial}{\partial t} n_k^d = \int \frac{dq}{2\pi} \int \frac{dk'}{2\pi} \int \frac{dq'}{2\pi} W_{k,q;k',q'} \delta\left(\epsilon_k^d + \epsilon_q^h - \left(\epsilon_{k'}^d + \epsilon_{q'}^h\right)\right) \times \delta_U(k+q-(k'+q'))\left(n_{k'}^d n_{q'}^h - n_k^d n_q^h\right), \quad \text{(B1)}$$

$$\frac{\partial}{\partial t} n_q^h = \int \frac{dk}{2\pi} \int \frac{dk'}{2\pi} \int \frac{dq'}{2\pi} W_{k,q;k',q'} \delta\left(\epsilon_k^d + \epsilon_q^h - \left(\epsilon_{k'}^d + \epsilon_{q'}^h\right)\right) \times \delta_U(k+q-(k'+q'))\left(n_{k'}^d n_{q'}^h - n_k^d n_q^h\right), \quad \text{(B2)}$$

where $\delta_U(k) = \sum_n \delta(k + n2\pi)$ as umklapp scattering can relax the momentum by multiples of the reciprocal lattice vector. The transition rate for hard-core collisions in one

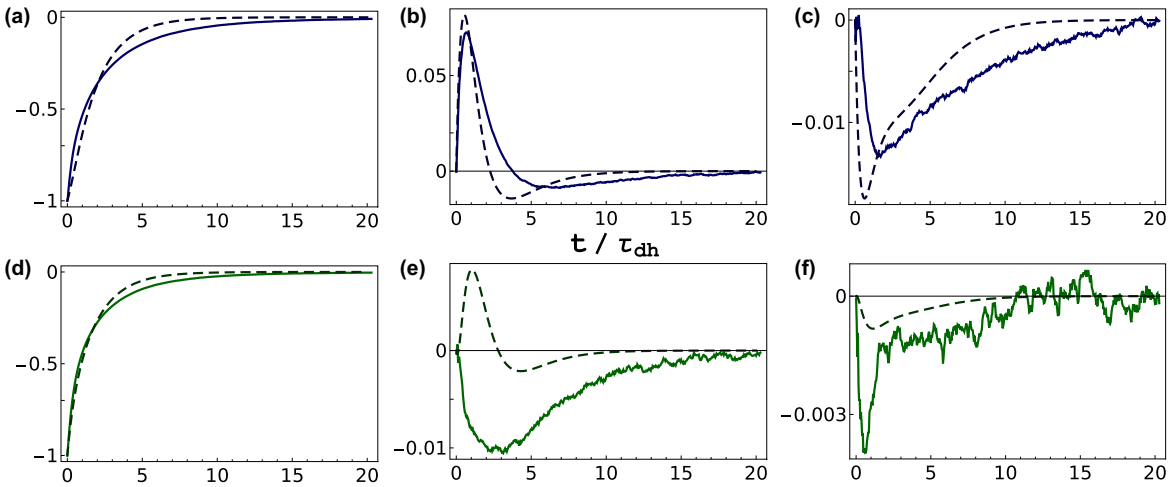


FIG. 6. (Color online) Relaxation of $\langle\cos(nk)\rangle$, $n = 2,4,6$, for doublons (a)–(c) and holons (d)–(f). Solid line, simulation data; dashed line, Boltzmann equation result.

dimension is exactly given by

$$W_{k,q;k',q'} = (2\pi)^2 \left|\partial_k \epsilon^d_k - \partial_q \epsilon^h_q\right| \left|\partial_{k'} \epsilon^d_{k'} - \partial_{q'} \epsilon^h_{q'}\right| \quad \text{(B3)}$$

This formula can, e.g., be obtained by calculating the change of $n^{d,h}_k$ from hard-core scattering with a neighboring particle and comparing the result with the Boltzmann formula. After using energy and lattice-momentum conservation and performing the Fourier series expansion of the distribution functions as

$$n^{d,h}_k = \sum_m \cos(mk)\, d_m / h_m \quad \text{(B4)}$$

we find the equations for the Fourier components

$$\begin{aligned}\frac{\partial}{\partial t} d_m = 2 \sum_{m',m''} d_{m'} h_{m''} \int \frac{dk}{2\pi} \int \frac{dq}{2\pi} \cos(mk) \left|\partial_k \epsilon^d_k - \partial_q \epsilon^h_q\right| \\ \times \{\cos(m' k_d) \cos[m''(k+q-k_d)] \\ - \cos(m' k) \cos(m'' q)\},\end{aligned}$$

$$\begin{aligned}\frac{\partial}{\partial t} h_m = 2 \sum_{m',m''} d_{m'} h_{m''} \int \frac{dk}{2\pi} \int \frac{dq}{2\pi} \cos(mq) \left|\partial_k \epsilon^d_k - \partial_q \epsilon^h_q\right| \\ \times \{\cos(m' k_d) \cos[m''(k+q-k_d)] \\ - \cos(m' k) \cos(m'' q)\},\end{aligned}$$

where $k_d(k,q)$ is the doublon momentum after the scattering of a doublon with momentum $k$ and a holon with momentum $q$, determined from energy and momentum conservation (modulo umklapp scattering).

We have solved Eqs. (B1) and (B2) numerically, including all modes up to $m = 8$, with the initial conditions $h_0(0) = d_0(0) = -h_2(0) = -d_2(0) = \rho$ and $h_m(0) = d_m(0) = 0$ otherwise, to match the initial condition $n^d_k(0) = n^h_k(0) = 8\,(J/U)^2 \sin^2 k$; see Fig. 2 of the main text. The result for the even modes (the odd modes are all zero) is compared in Fig. 6 to the simulation data. The Boltzmann equation predicts correctly the time scale of relaxation; see Figs. 6(a) and 6(d). As in $d = 1$ there is a high probability that one particle scatters again and again with the same scattering partner, a full quantitative agreement cannot be expected even for the first few scattering events.

For long times the Boltzmann equation predicts exponential relaxation as it does not capture thermal fluctuations of energy and particle density but describes those only on average.

## APPENDIX C: EQUILIBRIUM CORRELATION FUNCTION

Hydrodynamic long-time tails also dominate equilibrium correlation functions. In Fig. 7 we show $\langle e_i(t) e_i(0)\rangle_{\rm eq}$ obtained from a semiclassical simulation in equilibrium at $T = \infty$ where initially all doublons and holons have a $k$-independent momentum distribution $n^d_k = n^h_k = \text{const}$ and are uncorrelated in space. We assume the same density of doublons and holons. As for the quenches studied in the main text, it is difficult to extract reliably the long-time asymptotics due to large subleading corrections which vanish only slowly. The numerical data are equally well described by a power-law fit with exponent 0.59 and a fit to $c_1 t^{-1/2} + c_2 t^{-3/4}$ as expected from hydrodynamics.

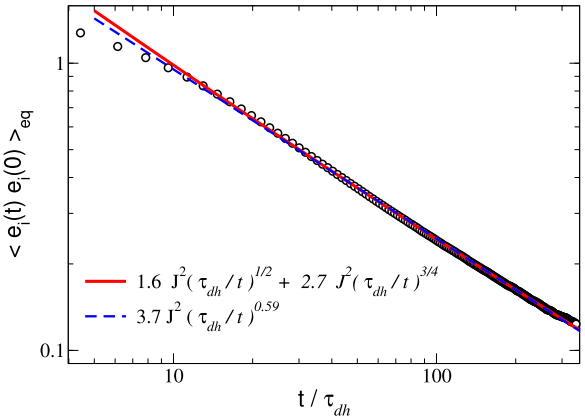


FIG. 7. (Color online) Correlation function $\langle e_i e_i(0)\rangle_{\rm eq}$ calculated in thermal equilibrium together with two fits to this function (see the legend), which equally well describe the numerical result.

[1] P. Calabrese and J. Cardy, Phys. Rev. Lett. **96**, 136801 (2006).
[2] C. Kollath, A. M. Läuchli, and E. Altman, Phys. Rev. Lett. **98**, 180601 (2007).
[3] M. Rigol, V. Dunjko, and M. Olshanii, Nature (London) **452**, 854 (2008).
[4] M. Moeckel and S. Kehrein, Phys. Rev. Lett. **100**, 175702 (2008).
[5] A. Polkovnikov, K. Sengupta, A. Silva, and M. Vengalattore, Rev. Mod. Phys. **83**, 863 (2011).
[6] A. Mitra and T. Giamarchi, Phys. Rev. Lett. **107**, 150602 (2011).
[7] M. Cheneau, P. Barmettler, D. Poletti, M. Endres, P. Schausz, T. Fukuhara, C. Gross, I. Bloch, C. Kollath, and S. Kuhr, Nature (London) **481**, 484 (2012).
[8] S. Trotzky, Y.-A. Chen, A. Flesch, I. P. McCulloch, U. Schollwöck, J. Eisert, and I. Bloch, Nat. Phys. **8**, 325 (2012).
[9] J. Berges, S. Borsányi, and C. Wetterich, Phys. Rev. Lett. **93**, 142002 (2004).
[10] M. Gring, M. Kuhnert, T. Langen, T. Kitagawa, B. Rauer, M. Schreitl, I. Mazets, D. A. Smith, E. Demler, and J. Schmiedmayer, Science **337**, 1318 (2012).
[11] M. Kollar, F. A. Wolf, and M. Eckstein, Phys. Rev. B **84**, 054304 (2011).
[12] A. Mitra, Phys. Rev. B **87**, 205109 (2013).
[13] M. Marcuzzi, J. Marino, A. Gambassi, and A. Silva, Phys. Rev. Lett. **111**, 197203 (2013).
[14] R. A. Barankov, L. S. Levitov, and B. Z. Spivak, Phys. Rev. Lett. **93**, 160401 (2004).
[15] E. A. Yuzbashyan, O. Tsyplyatyev, and B. L. Altshuler, Phys. Rev. Lett. **96**, 097005 (2006).
[16] M. Eckstein, M. Kollar, and P. Werner, Phys. Rev. Lett. **103**, 056403 (2009).
[17] M. L. R. Fürst, C. B. Mendl, and H. Spohn, Phys. Rev. E **88**, 012108 (2013).
[18] M. Tavora and A. Mitra, Phys. Rev. B **88**, 115144 (2013).
[19] M. Stark and M. Kollar, arXiv:1308.1610.
[20] A. Rapp, S. Mandt, and A. Rosch, Phys. Rev. Lett. **105**, 220405 (2010).
[21] J.-S. Bernier, D. Poletti, P. Barmettler, G. Roux, and C. Kollath, Phys. Rev. A **85**, 033641 (2012).
[22] L. D. Landau and E. M. Lifshitz, *Fluid Mechanics*, 2nd ed., Course of Theoretical Physics Vol. 6 (Pergamon Press, Oxford, 1987).
[23] S. Mukerjee, V. Oganesyan, and D. Huse, Phys. Rev. B **73**, 035113 (2006).
[24] M. Kardar, G. Parisi, and Y.-C. Zhang, Phys. Rev. Lett. **56**, 889 (1986).
[25] M. Prähofer and H. Spohn, J. Stat. Phys. **115**, 255 (2004).
[26] H. van Beijeren, Phys. Rev. Lett. **108**, 180601 (2012).
[27] H. Spohn, arXiv:1305.6412.
[28] P. Grassberger, W. Nadler, and L. Yang, Phys. Rev. Lett. **89**, 180601 (2002).
[29] M. Greiner, O. Mandel, T. Esslinger, T. Hansch, and I. Bloch, Nature (London) **415**, 39 (2002).
[30] M. Garst and A. Rosch, Europhys. Lett. **55**, 66 (2001).
[31] P. Barmettler, D. Poletti, M. Cheneau, and C. Kollath, Phys. Rev. A **85**, 053625 (2012).
[32] S. Sachdev and K. Damle, Phys. Rev. Lett. **78**, 943 (1997).
[33] H. Rieger and F. Iglói, Phys. Rev. B **84**, 165117 (2011).
[34] P. Cipriani, S. Denisov, and A. Politi, Phys. Rev. Lett. **94**, 244301 (2005).
[35] L. Delfini, S. Denisov, S. Lepri, R. Livi, P. K. Mohanty, and A. Politi, Eur. Phys. J.: Spec. Top. **146**, 21 (2007).
[36] N. Strohmaier, D. Greif, R. Jördens, L. Tarruell, H. Moritz, T. Esslinger, R. Sensarma, D. Pekker, E. Altman, and E. Demler, Phys. Rev. Lett. **104**, 080401 (2010).
[37] B. Bauer *et al.*, J. Stat. Mech. (2011) P05001.
[38] R. Kubo, M. Yokota, and S. Nakajima, J. Phys. Soc. Jpn. **12**, 1203 (1957).